Journal of Marine Research, 49, 411–434, 1991

The climatological seasonal circulation of the Mediterranean Sea

by Eli Tziperman[1] and Paola Malanotte-Rizzoli[2]

ABSTRACT

The horizontal circulation of the upper 800 m of the Mediterranean Sea is calculated from a seasonal climatological hydrographic data set using a simple inverse model. The results show a fairly steady surface circulation in the western Mediterranean and a somewhat stronger seasonal signal in the surface circulation of the eastern Mediterranean. The deep flow field can be calculated for most of the Mediterranean, except for the Levantine basin east of Crete, where the high noise level in the data masks the deep circulation. The calculated deep velocity field (below 500 m) shows some interesting features, including several steady cyclonic gyres in the West Mediterranean and in the Ionian basin of the East Mediterranean. In particular, the path of Levantine Intermediate water from the straits of Sicily toward the straits of Gibraltar is found to be along the Sardinian, French and then Spanish and Majorca coasts, and not directly along the African coast. The robustness of the inverse model results for the deep velocity field is demonstrated by examining several variations of the model (with and without mixing, different initial reference levels, etc). The model also calculates long- and cross-isopycnal mixing coefficients for the temperature and salinity but the error bars calculated for these parameters are large, and they are found not to be significantly different from zero.

1. Introduction

The physical oceanography of the Mediterranean Sea (Fig. 1) has been studied for many years now (detailed reviews of the present knowledge of the East Mediterranean (EM) and the West Mediterranean (WM) were given by Malanotte-Rizzoli and Hecht (1988) and Hopkins (1988), respectively). Yet existing studies of the Mediterranean Sea often conflict as shown by the above mentioned reviews, and there are still quite a few unresolved issues concerning its dynamics, circulation, and water mass formation processes. Some of these issues are the general pattern of the general circulation of the EM; the strength of the seasonal signal in the EM compared to that of the WM; the structure of the deep circulation in both parts of the sea; the seasonal variability of the inflow of Atlantic water from the WM to the EM through the Sicily

1. Environmental Sciences and Energy Research, The Weizmann Institute of Science, Rehovot 76100, Israel.

2. Department of Earth, Atmospheric and Planetary Sciences, Massachusetts Institute of Technology, Cambridge, Massachusetts, 02139, U.S.A.

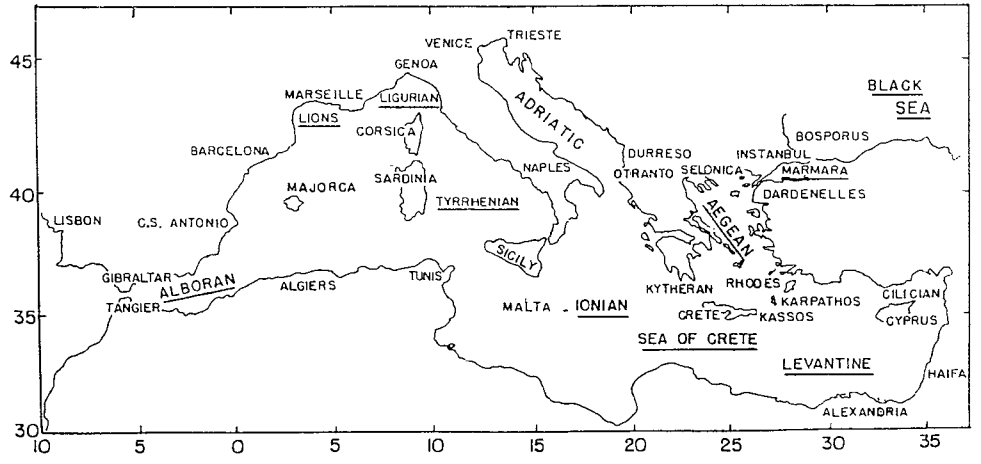

Figure 1. Morphology of the Mediterranean Sea.

straits; the path of the Levantine Intermediate Water from its formation sites in the EM to the straits of Gibraltar; and more.

The purpose of this work is to present the circulation of the upper 800 m of the Mediterranean Sea for all four seasons, as calculated from a climatological hydrographic data base, using a simple inverse model. More specifically, we wish to address three main issues. First, we examine the seasonal signal in the surface circulation of the Mediterranean Sea, and try to determine the areas in which the circulation is steady and those in which the seasonal signal has significant magnitude. Second, we wish to calculate the deep circulation of the entire Mediterranean Sea that is still not well known. Finally, we want to try and make progress toward a better definition of the general circulation of the East Mediterranean. Such a definition is needed because the circulation of the EM is dominated by small sub-basin gyres, and it is often not entirely clear which of the gyres calculated from a given data set are permanent (or seasonal) and which are only transient mesoscale features.

One can point out three main difficulties that were commonly encountered in previous efforts to calculate the general circulation of the Mediterranean Sea: (a) previous studies were often based on regional or sparse hydrographic data sets and usually gave an incomplete spatial or temporal coverage of the circulation; (b) aliasing by the small and strong mesoscale eddies often made it difficult to resolve the features of the general circulation, and (c) the somewhat arbitrarily assumed level of no motion resulted in an uncertain deep circulation which is quite sensitive to the choice of the level of no motion.

In order to overcome these problems in the present work we have taken the following steps. (a) We use a seasonal climatological hydrographic data set, covering the whole Mediterranean Sea, and given for all four seasons. These data provide a fairly good temporal and spatial coverage of the entire Mediterranean Sea. The

resolution of the hydrographic data is half a degree longitude and latitude, and it is given in 17 levels from the surface to 800 m deep. (b) The data are smoothed by objective mapping to reduce the problem of aliasing by mesoscale eddies. (c) An inverse model is used to calculate the absolute velocity field, avoiding the undesired assumption of level of no motion.

The circulation calculated using these data and methodology enables us to try and resolve some of the many unknown aspects of the circulation of the Mediterranean Sea. In particular, the use of inverse method proves to be worthwhile in calculating the deep circulation, as it reveals some very interesting deep features. Our results also provide a climatological basis for comparison with the analysis of the new quasi-synoptic hydrographic data recently available from the POEM program in the EM (Malanotte-Rizzoli and Robinson, 1988).

In the following sections the climatological data base used for this study is described (2), and then the details of the inverse model used are given (3). The calculated climatological horizontal geostrophic circulation of the Mediterranean at 10 m and at 700 m, for all four seasons, is presented in Section 4. The results are critically examined and some technicalities are discussed in Section 5, and we conclude in Section 6.

2. The data

The data base for this study is the Mediterranean part of the "Master Generalized Digital Environmental Model" (GDEM) gridded hydrographic data base (Naval Oceanographic Office, 1989; Davis *et al.,* 1986). The data are of temperature and salinity for the four seasons (where each season is taken to be three months long, with winter defined from January to March, spring from April to June, etc), given on a half degree longitude by half degree latitude horizontal resolution, and in 17 vertical levels (0, 10, 20, 30, 50, 75, 100, 125, 150, 200, 250, 300, 400, 500, 600, 700 and 800 meters deep).

The GDEM is a gridded data set obtained from the original hydrographic data by a fairly complex mapping procedure (see above references). Examining the temperature and salinity fields it was found that there is still a significant level of grid-scale noise in the data. In order to remove this noise while not introducing large-scale tendencies that were not present in the data originally, we have smoothed the data by objective mapping (Bretherton *et al.,* 1976) in the following manner. Each level was mapped separately, using a large variance level (100%), and an exponential correlation function with a correlation distance of 150 km. To prevent the artificial creation of large-scale tendencies in the mapped fields, only points within an influence circle of the nearest neighboring grid points (total of nine nearest grid points) are used when mapping the fields at a given grid point. When used this way the objective mapping was found to completely remove any feature that was represented by one grid point only, but it did not seem to introduce large-scale features which did not

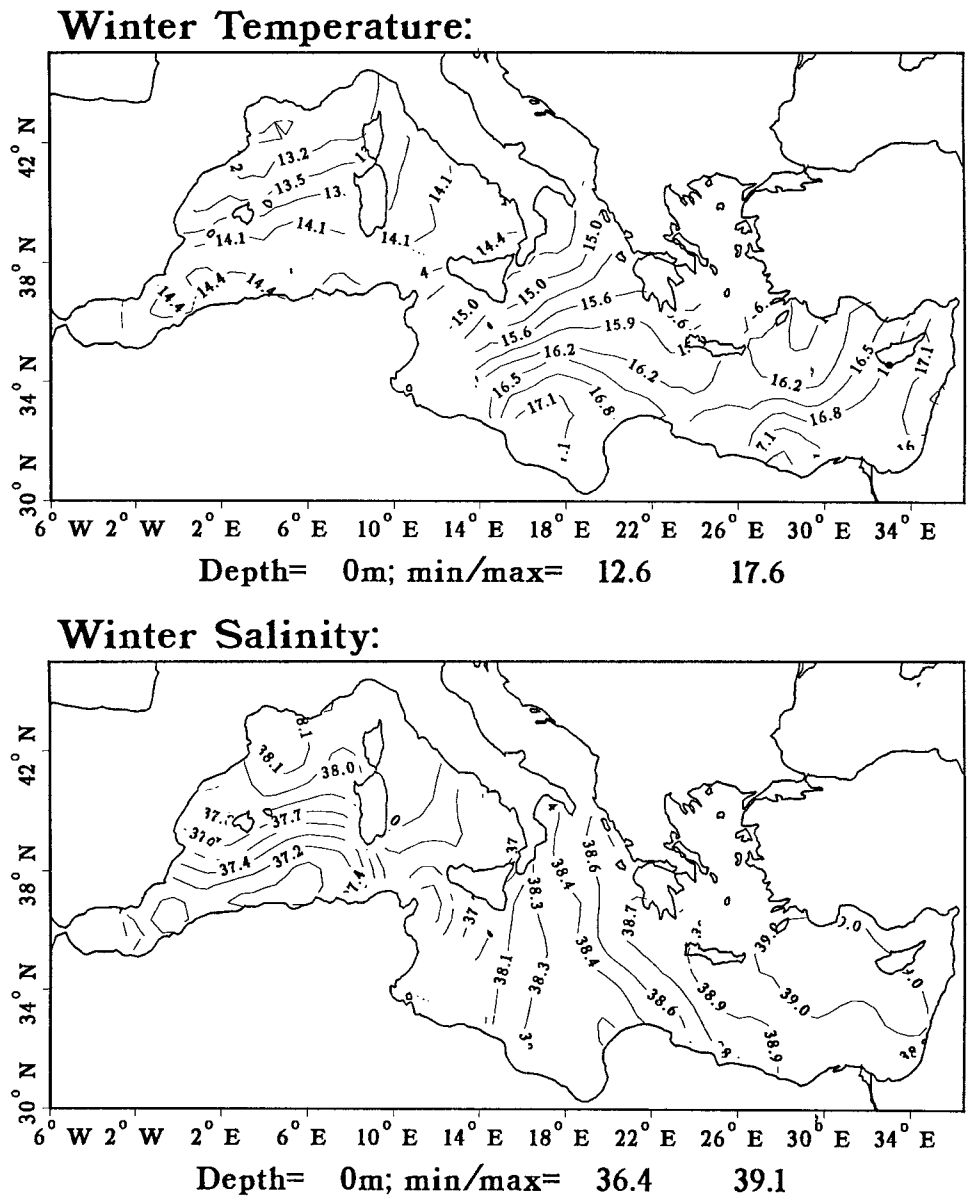

Figure 2. Surface temperature and salinity during the winter season (after objective mapping, see Section 2).

exist in the data. The use of climatological data does cause weakening of the geostrophic velocities and spreading of narrow currents, and this should be noted when comparing the present results to those obtained from quasi-synoptic data. Figures 2 and 3 show the surface temperature and salinity during the winter and summer seasons, after the smoothing by the objective mapping.

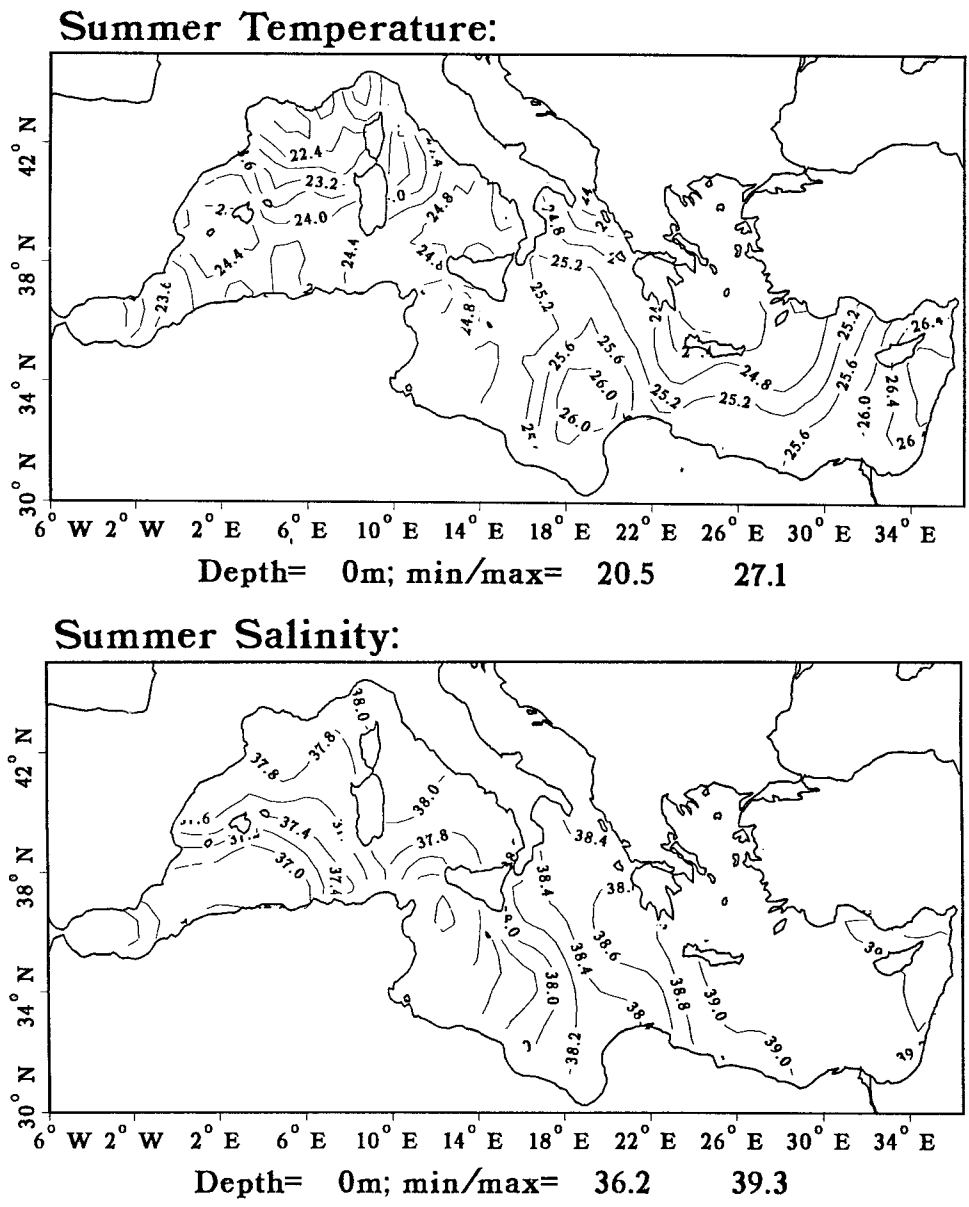

Figure 3. Surface temperature and salinity during the summer season (after objective mapping, see Section 2).

The use of mapped and gridded hydrographic data is essential in a linear inverse study such as the present one, as the original station data is non-uniformly distributed in time and space. Unfortunately the mapping process is known to affect the data through the smoothing of smaller scale features etc, as explained above. A

possible remedy to the problems caused by the mapping is to allow the inverse calculation to solve for the optimal hydrography, consistent both with the data and with the model dynamics. This can be achieved by nonlinear inverse methods (e.g. Tziperman and Thacker, 1989). These methods, however, are quite new to oceanography, so that at present we prefer to restrict ourselves to the linear methodologies, which we believe can still be used to enhance our knowledge of the Mediterranean circulation.

3. The inverse model

The inverse model used here is based on the model described in detail by Tziperman and Hecht (1988, hereafter TH). It is also similar to the β-spiral inverse model used by Olbers *et al.* (1985). The model is described in this section, while in Section 5 we examine the robustness of its results to some of the assumptions made in this section during model formulation. Readers not interested in the more technical details may now skip to Section 4 where the results are described.

a. Model equations

Beginning with the model formulation, we first use the thermal wind equations to write the velocity field as a sum of reference and geostrophic velocities

$$u(x,y,z) = u_0(x,y) + \int_{z_0}^{z} \frac{g}{\rho_0 f_0} \rho_y dz', \quad v(x,y,z) = v_0(x,y) + \int_{z_0}^{z} \frac{-g}{\rho_0 f_0} \rho_x dz'$$
$$w(x,y,z) = w_0(x,y), \tag{1}$$

where $u_0(x,y) = u(x,y,z_0)$, v_0 and w_0 are the unknown velocities at the reference level z_0. Gravity is denoted by g, f_0 is the Coriolis parameter, and ρ_0 is a constant reference density. Note that the vertical velocity is assumed depth independent, and is also an unknown to be calculated by the inverse model (the choice of a depth independent vertical velocity was discussed in detail and justified by TH).

Next, the advection-diffusion equations for the temperature and salinity are used to form a linear set of equations for the model unknowns (reference velocities and mixing coefficients). The properties of the upper 200–300 m in the Mediterranean Sea are strongly seasonal, but below about 300 m the temperature and salinity are at a steady state to a very good approximation. This steadiness of the deep water in the Mediterranean is known from previous studies, and was checked using the present data set by comparing the deep data for the different seasons. Because the deep fields are steady, they may be assumed to be governed by a steady state advection diffusion equation. This steady state equation is therefore used to solve for the unknown reference velocities and other model unknowns. Once the solution for the velocity field is calculated by the inverse, we should verify that the deep velocities are indeed at a steady state consistent with our assumptions, and this is done in Section

5. (Note that the geostrophic equations, unlike the tracer equations, are used also near the surface for the calculation of the geostrophic velocities. The geostrophic approximation holds, of course, to a good approximation even if the surface temperature, salinity and velocities vary with the seasonal cycle.) Parameterizing the mixing processes by tensor diffusivities to adequately separate long- and cross-isopycnal mixing (Redi, 1982; Olbers *et al.,* 1985), the steady state advection diffusion equations are

$$uT_x + vT_y + wT_z = \partial_i[\kappa_{ij}\partial_j T] \tag{2}$$

and a similar equation for the salinity, where the diffusivity tensor is

$$\kappa_{ij} = A_l\delta_{ij} + (A_c - A_l)\frac{(\partial_i\sigma)(\partial_j\sigma)}{|\nabla\sigma|^2}. \tag{3}$$

The potential density is denoted by σ, and ∂_i ($i = 1, 2, 3$) is the derivative with respect to the three spatial coordinates. The long- and cross-isopycnal mixing coefficients A_l and A_c are unknowns solved by the inverse. They are calculated separately at each horizontal position and are therefore allowed to vary freely in the horizontal. In addition, for representing their vertical structure, the coefficients were expanded in Chebyshev polynomials in the vertical coordinate (see TH, where the horizontal and vertical mixing coefficients used there are also allowed to be a function of depth in a similar manner). In the calculations presented here, a third order Chebyshev polynomial was used, giving a vertical resolution of 800 m/3 or about 300 m for vertical variations in the mixing coefficients.

The velocity field (1) is substituted into the advection diffusion equations (2) for the temperature and salinity fields to obtain a set of linear equations for the unknown reference velocities and mixing coefficients. The temperature and salinity equations (2) were evaluated at five deep levels (300, 400, 500, 600 and 700 m), giving 10 equations for the model unknowns at any given horizontal location (except in a few locations shallower than 800 m). The initial reference level (z_0 in (1)) was chosen to be 700 m. In Section 5 we demonstrate that the inverse results for the horizontal velocity field are not sensitive to the choice of the initial reference level. The equations are written in matrix form,

$$A\mathbf{b} = \Gamma, \tag{4}$$

where $\mathbf{b}$ is the vector of unknowns containing the three reference velocities and the Chebyshev coefficients in the expansion of the mixing coefficients A_c and A_l; A and Γ are known matrix and vector containing derivatives of the temperature and salinity fields. The above linear system is solved by singular value decomposition (SVD) (Wunsch, 1978). It is also possible to add a set of linear inequalities requiring the mixing coefficients to be positive as described by TH. But the model does not resolve the mixing coefficients (as discussed in Section 5), and the solution for these

parameters seems to be controlled by the noise in the data. There was no point, therefore, in applying positivity constraints to the calculated coefficients, as the results for the coefficients are not significantly different from zero in any case. It is important to note, however, that the solution for the horizontal velocity field did not depend on the specific form of the parameterization of mixing chosen. In Section 5 we show that the horizontal velocity field does not change very much even when no mixing is included in the temperature and salinity equations, and we discuss in more detail the role of mixing in the model.

Before applying the SVD procedure to solve for the unknowns, each of the equations (4) was weighted by the vertical spacing of grid points at the level where the equation was evaluated. This is equivalent to the standard weighting by the thickness of the layers in the box inverse described by Wunsch, (1978), where the importance of such weighting is discussed. This form of weighting is probably the best choice in cases such as ours, where no information is available on the dependence of the error in the data on depth (or location). (When error information is available, each equation is also weighted by its inverse squared error.)

b. Comments

Spatial derivatives in the above equations are evaluated using standard center differences. In order to be able to evaluate the equations and calculate geostrophic velocities at the grid points nearest to the coast, the temperature and salinity are extrapolated to cover an additional point on the coast. These additional points are then used to evaluate the center differences at the grid points nearest to land in the original data. This procedure is similar to the extrapolation done in standard dynamic calculations where the shallower of two hydrographic stations is often extrapolated to the depth of the deeper one, in order to calculate the geostrophic velocity perpendicular to the section between the two stations. In Section 5 we show an inverse calculation based on nonextrapolated data in order to demonstrate that the extrapolation does not introduce any artificial circulation near the boundaries.

A comment on the gridded data used here is due before we proceed to present the inverse results. The use of gridded climatological data, based on many different observations taken over many years, has some obvious advantages in allowing the investigation of seasonal effects, providing a complete spatial coverage of the Mediterranean Sea, removing aliasing by mesoscale eddies etc. There is an obvious trade-off between resolution of the gridded data set and the number of original measurements used to calculate the average at any particular grid point. At half a degree resolution it seems that the averaging removed most of the aliasing by eddies etc, but such a resolution does not allow a detailed calculation of the currents in narrow straits and in some coastal regions. Only two to three grid points are available to span the width of the Alboran Sea adjacent to the Gibraltar Straits, for example, and one cannot expect the results to properly describe the various small gyres known

to exist in that region. Similarly, the insufficient resolution near the coast often masks parts of gyres there. One occasionally has to decide subjectively or based on previous knowledge of the circulation, whether a half-gyre seen near the coast should close in the unresolved area adjacent to the coast, or whether it is a part of an undulating current flowing along the coast.

Compiling the climatological data on a higher resolution grid may not be a good solution for this problem, as it would reduce the number of observations used to obtain the average hydrography at each grid point, and therefore increase the noise level that seems already non-negligible for these data. In any case, our results indicate that the half degree resolution data provide a good description of the interior sub-basin scale circulation of the Mediterranean Sea, while results near the coast or in narrow straits should be taken with a grain of salt.

A related problem has to do with the fact that the inverse model that we use is local, and therefore the calculated flow field does not necessarily satisfy mass conservation (a problem shared by other beta spiral methods, e.g. Olbers *et al.,* 1985). This problem is amplified by the complex geometry of the Mediterranean and the poor resolution near the coasts, and there are several cases in which the calculated solution for the horizontal velocity field clearly misses parts of gyres that should close near the coast. We try to point out these problems while describing the results in the following section.

Overall, however, the performance of the inverse model with this particular data set is quite satisfactory; and the results, especially in the interior and deeper parts of the Mediterranean, contribute to our knowledge of the physical oceanography of the Mediterranean Sea. We now proceed to describe the results of the inverse calculation for the horizontal velocity field. The inverse model also calculates eddy mixing coefficients and vertical velocities and these results are discussed in Section 5.

4. The climatological seasonal circulation of the Mediterranean Sea

We have chosen to present the calculated horizontal circulation of the Mediterranean Sea by showing the circulation at the depths of 10 m and 700 m (Figs. 4–7). The upper circulation is first briefly described, then the deeper, and then the vertical structure of the circulation in the upper 800 m is discussed.

a. The upper circulation

i. West Mediterranean. The surface circulation of the West Mediterranean, as represented by the maps shown here for the depth of 10 m, is quite steady during the four seasons, although somewhat more intensified during the winter.

The various gyres one expects to find in the Alboran Sea east of the Gibraltar Straits (Hopkins, 1988) are not properly resolved by the half degree resolution of the data. Our results begin showing a coherent pattern of circulation west of about 0E, where the Atlantic Water flows northward, presumably due to the break in the

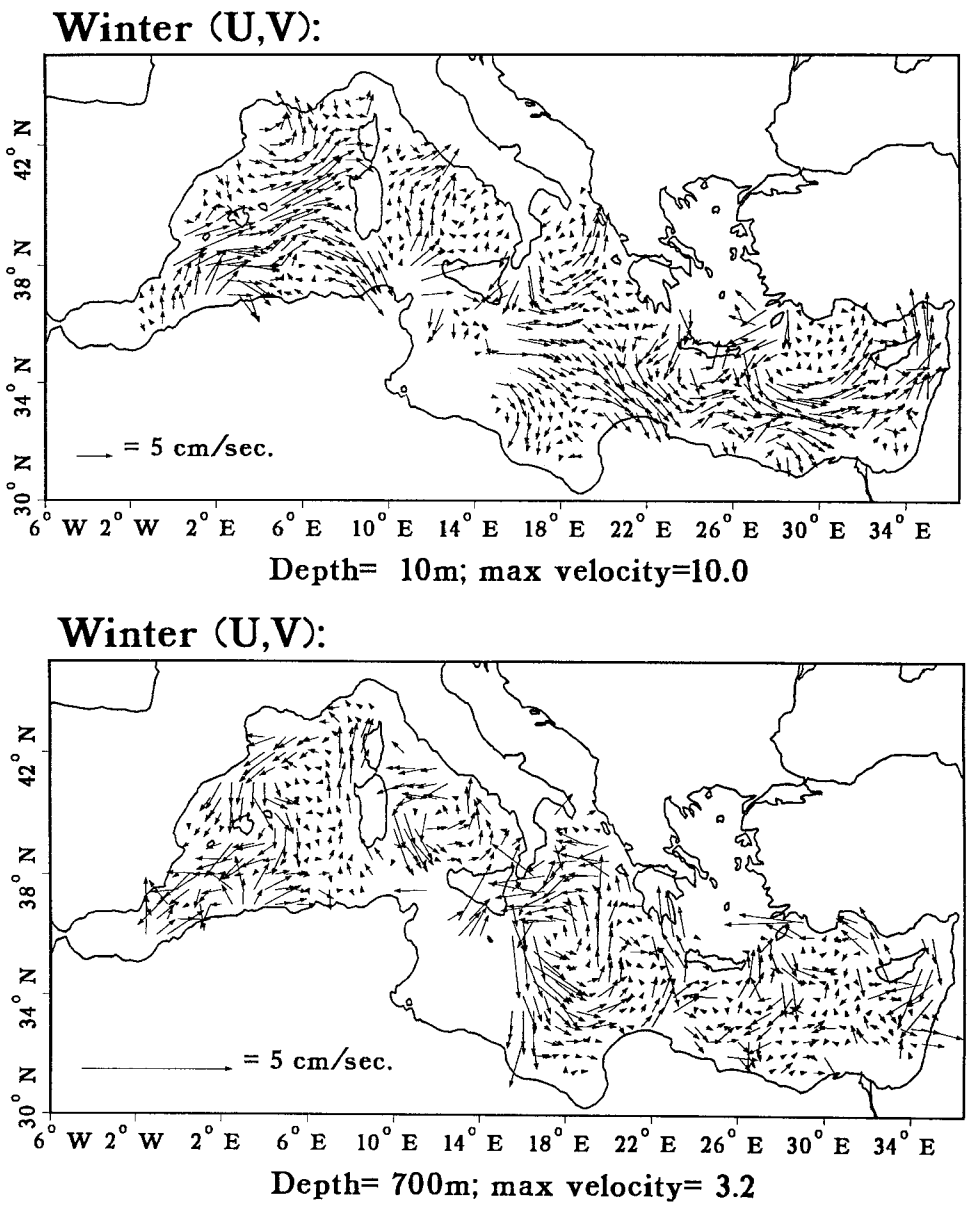

Figure 4. The winter circulation shown at the depths of 10 m (upper panel) and 700 m (lower). Note that the scale for the velocity vectors is different for the two levels shown (see reference arrow at lower left corner).

Moroccan coast, and then breaks into two branches. The turning northward of the Atlantic Water (AW) is similar to that calculated by Alain (1960), but is different from the classic picture in which the AW flows along the coast until reaching Sardinia. The first of the two branches of the circulation returns southward toward

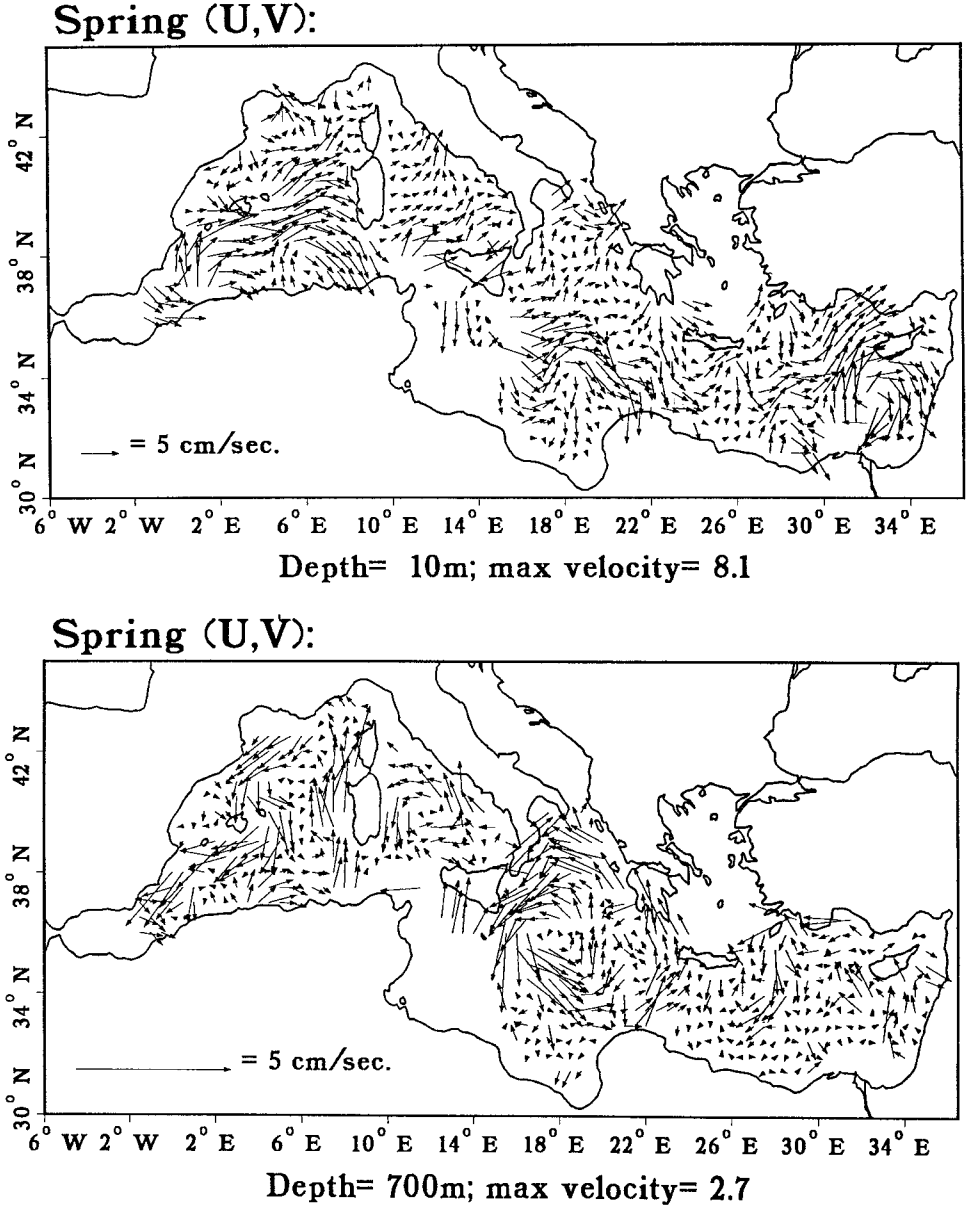

Figure 5. As in Figure 1 for the spring.

the African coast, and the second continues eastward, toward Sardinia. The northern branch splits before Sardinia into several weaker flows to the passage south of Sardinia, to the Ligurian Sea north of Corsica, and a third branch that recirculates in the Lions Bay (this is one location where the ½° resolution of our data was not sufficient to resolve the part of the gyre that is known to close near the coast in the

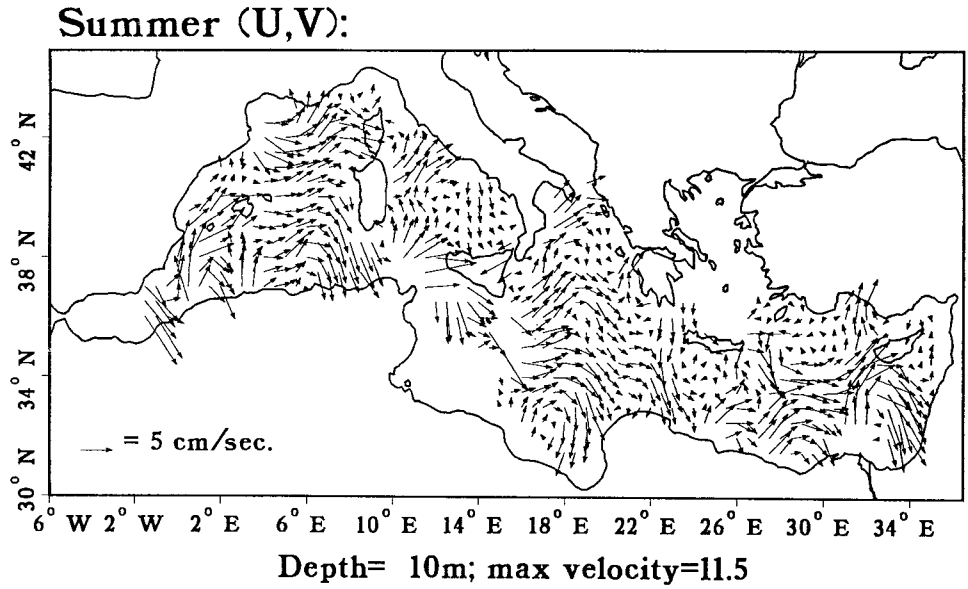

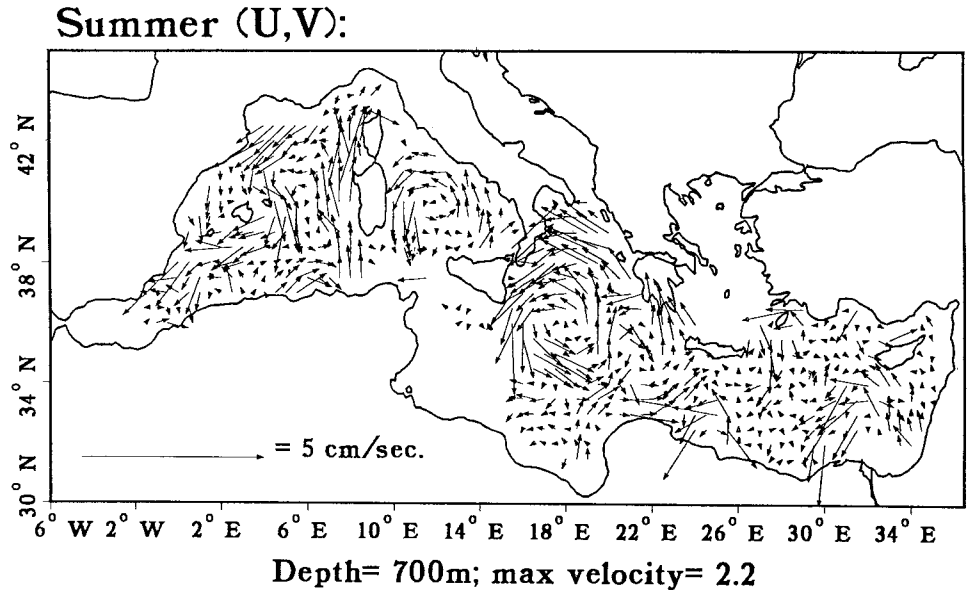

Figure 6. As in Figure 4 for the summer.

Gulf of Lion). The relative strength of each of these flows changes from season to season, but not to a large extent. The south branch of the Atlantic Water that broke off near the exit from the Alboran Sea continues along the African coast, passing through an anticyclonic gyre (or perhaps a strong undulation) at about 5E, and then flows eastward through the Sardinian passage. After passing Sardinia, part of the

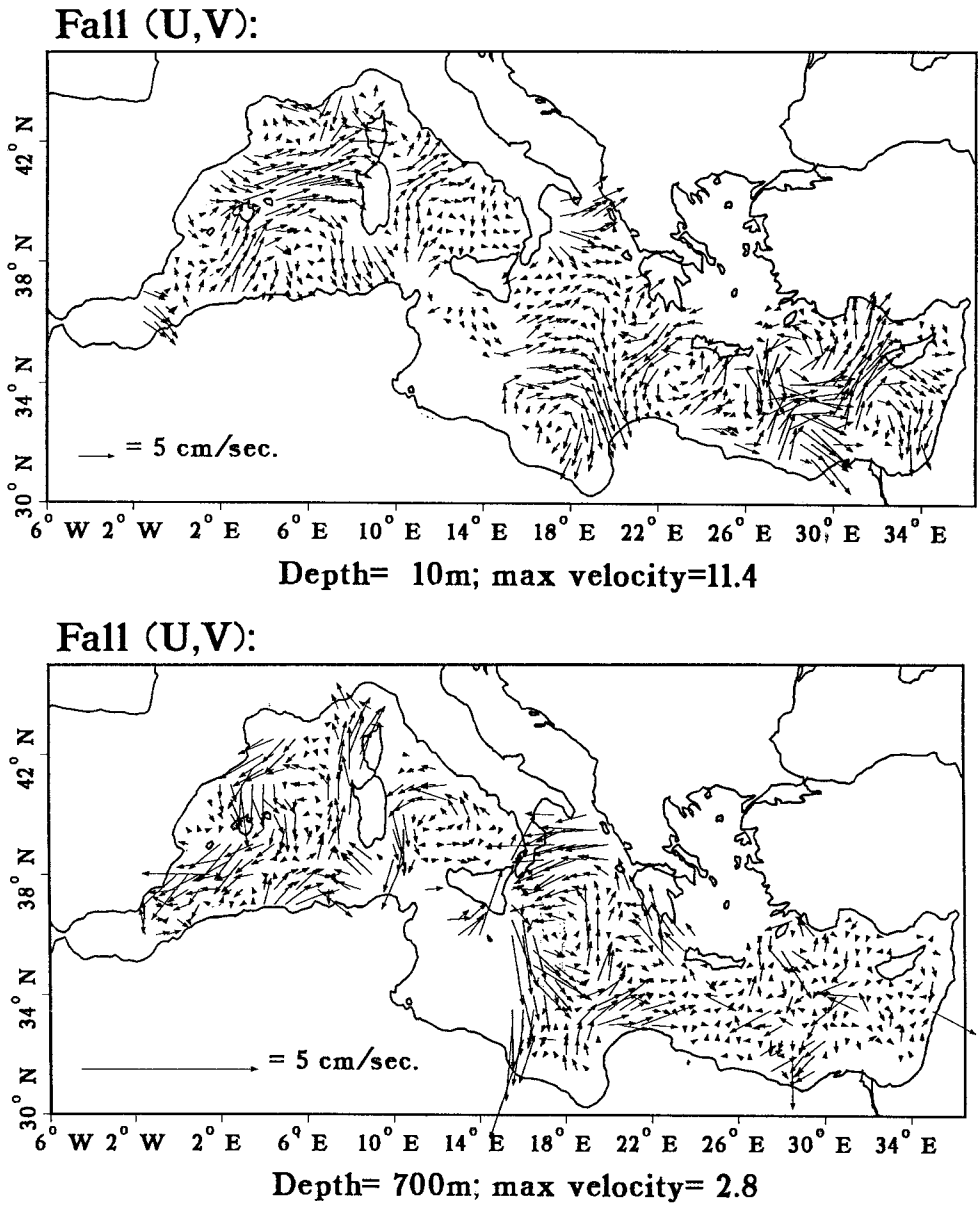

Figure 7. As in Figure 4 for the fall.

flow turns northward into the Tyrrhenian Sea, and the rest continues through the Sicily Straits into the Eastern Mediterranean.

ii. East Mediterranean. The seasonal signal of the East Mediterranean upper circulation as seen in Figures 4–7 is somewhat stronger than that of the West Mediterra-

nean, as may be expected by examining the strong seasonal signal in the forcing by the wind and heat fluxes at the surface (May, 1982). The flow through the Sicily Straits itself is again not very well resolved by the present data. Once past the straits, however, the flow can be seen continuing south-eastward into the Ionian Sea.

In all seasons except winter the inflow of Atlantic Water from the Sicilian Straits forms a meander that extends from about 15E to the eastern tip of the Gulf of Sidra (20E). This interesting dynamic feature may be related to the interaction of the eastward flow with the topographic or planetary β effects, and its disappearance in the winter seems related to the change in wind curl in the Ionian Sea at that time (May, 1982). In the northern part of the Ionian Sea, the surface circulation is again seasonal. It changes from a cyclonic gyre in the winter, to a north eastward flow of a branch of the entering Atlantic Water in the summer. This branch of the Atlantic Water later returns southward and joins the main flow from the straits of Sicily toward the Levantine basin.

East of the Ionian Sea, in the Sea of Crete, the calculated circulation is quite noisy. Yet, it is possible to identify a coherent cyclonic circulation pattern between Crete and the African coast that seems to be there at all seasons. Consider next the surface circulation in the Levantine basin, east of Crete. In the northwestern part of this basin, southeast of Rhodes and extending eastward, there is a strong cyclonic gyre that can be identified at all four seasons. Its size changes from season to season, occupying the region between Crete and Cyprus some of the time, and shrinking toward Rhodes at other times. The strong bottom topography of the deep Rhodes basin east of the island of Rhodes is believed to be responsible for the fairly strong and consistent gyre found there (Malanotte-Rizzoli and Hecht, 1988; Anati, 1984). Farther eastward, south of Cyprus, there is a strong and fairly steady anticyclonic gyre that can be identified at all seasons except for winter. This gyre can often be seen in data regularly collected in the region during recent years (Hecht *et al.,* 1988). Finally, north of the Egyptian coast, at about 28E, there is a half gyre seen near the coast that should probably close in the coastal area not resolved by the present data. This gyre can also be seen in some of the POEM data obtained recently (Ozsoy *et al.,* 1989).

The complex topography and geometry of the East Mediterranean basin tend to induce a general circulation that is composed of several small sub-basin gyres. But when calculating such sub-basin gyres from quasi-synoptic data there is always the possibility that they are mesoscale features and not necessarily a part of the permanent or seasonal circulation. However, the presence of the two gyres south of Cyprus and north of the Egyptian coast in the circulation calculated here from climatological data indicates that they may probably be considered a part of the general circulation of the East Mediterranean.

It is difficult to compare the above circulation to that found by previous studies of the EM, as these often contradict (Malanotte-Rizzoli and Hecht, 1988). According

to the classic circulation picture for the region one expects to see the Atlantic Water flowing eastward along the African coast, then northward to the Turkish coast, and returning westward along the northern coast of the Levantine basin. This is obviously not what we find here, and in fact the more recent POEM data also seem to indicate that the circulation in the Levantine basin is not as steady as it was thought to be (Robinson *et al.,* 1987; Tziperman and Hecht, 1988). In the present calculation one can see a general eastward flow in the southern Levantine basin, together with the various small gyres described above. The flow is certainly not steady, although the seasonal variability seems mostly limited to the Ionian basin and the easternmost part of the Levantine basin. In any case, the noisy circulation calculated in some areas of the EM clearly demonstrates the need to obtain and analyze better data sets for the Levantine basin.

b. The deeper circulation

The deeper circulation is represented here by the velocity maps for the depth of 700 m (Figs. 4–7). The calculation of this deeper circulation is where the inverse model proves very useful. The velocities calculated by the inverse model at the initial reference level at 700 m are fairly weak and the circulation of the surface water can therefore be calculated to a good approximation by using dynamic calculations with a reasonably deep reference level. The situation is different, however, if one is interested in the deeper circulation. Here an arbitrary choice for the reference level may result in a completely wrong circulation. In fact, several interesting features of the deep circulation at 700 m that can be seen in Figures 4–7, would obviously not show up had we used an arbitrary deep level of no motion at that depth. The results shown here for the circulation at 700 m were found to be independent of the initial choice of level of no motion in our calculation, as discussed in detail in Section 5.

i. West Mediterranean. A most interesting feature of the deep circulation is the cyclonic circulation made up of the northward flow along the Sardinian coast, and the south westward flow along the Spanish and Majorca coast. The two seem to be connected by a flow along the French coast, although this flow is not fully resolved by the data there. This flow, intensified near the coasts and fairly narrow, is most probably the flow of Levantine Intermediate Water flowing from the eastern Mediterranean toward the Straits of Gibraltar. The LIW takes the longer route to Gibraltar, turning to the right after entering the WM, and flowing along the west coast of Sardinia, perhaps due to the influence of the Coriolis force. This result is similar to the flow described by Wüst (1961) for intermediate depths using the core method, and following maximum salinity contours. But this route of the LIW in the WM is only one of several possible ones discussed in the literature (Hopkins, 1988), and our results clearly support the longer route described above as opposed the direct one along the African coast. Another steady deep feature that can be seen in

the West Mediterranean is a deep cyclonic circulation in the Tyrrhenian Sea, between Italy to the east and Sardinia to the west.

ii. Eastern Mediterranean. The most noticeable deep feature in the Eastern Mediterranean is the cyclonic circulation occupying most of the Ionian Sea. This steady feature is particularly interesting because of the strong seasonal variability of the surface circulation in this region, which obviously does not penetrate into the deep sea. Finally, in the Levantine basin east of Crete, the calculated velocity at the initial reference level at 700 m is noisy and random, and is below the noise level (see Section 5 for a discussion of the error estimates).

c. The vertical structure of the horizontal circulation

By examining the horizontal velocity field for all the levels from the surface to 800 m, (not shown here) the vertical extent of the surface and deep circulation features discussed above can be determined. In general, we found that the surface circulation of both the West and the East Mediterranean extends down to about 250 or 300 m, while the deep features discussed above start at about 500 m or 600 m, and extend down to (at least) the maximum depth of our data, 800 m. If a level of no motion that best represents both the surface and deep circulations is to be chosen according to these results, it should be at around 400 m deep.

5. Critical evaluation of the inverse results

In this section, the robustness of the results presented in Section 4 is demonstrated, the inability of the model to calculate mixing coefficients and vertical velocities is discussed, and the resolution and error information that can be used to evaluate the inverse solution are examined.

i. Robustness. We first demonstrate the robustness of the deep circulation calculated by the inverse model. This is done by examining the results of the inverse calculation for a variety of models, different only by one aspect at a time, and making sure that the results shown in the previous section are not sensitive to each particular aspect of the model.

We begin with the choice of the initial level of no motion for the inverse calculation. Figure 8 shows the absolute (geostrophic plus reference velocities) winter circulation at 700 m, obtained by using a reference level of 400 m instead of 700 m for the calculation of the relative geostrophic velocities [$z_0 = 400$ m in (1)]. Comparing the circulation to that of Figure 4, it is clear that the solution for the absolute velocity is not sensitive to the initial choice of level of no motion.

Next, consider the effect of the mixing parameterization used in the inverse model. Figure 9 shows the winter circulation at 700 m obtained using the same inverse model

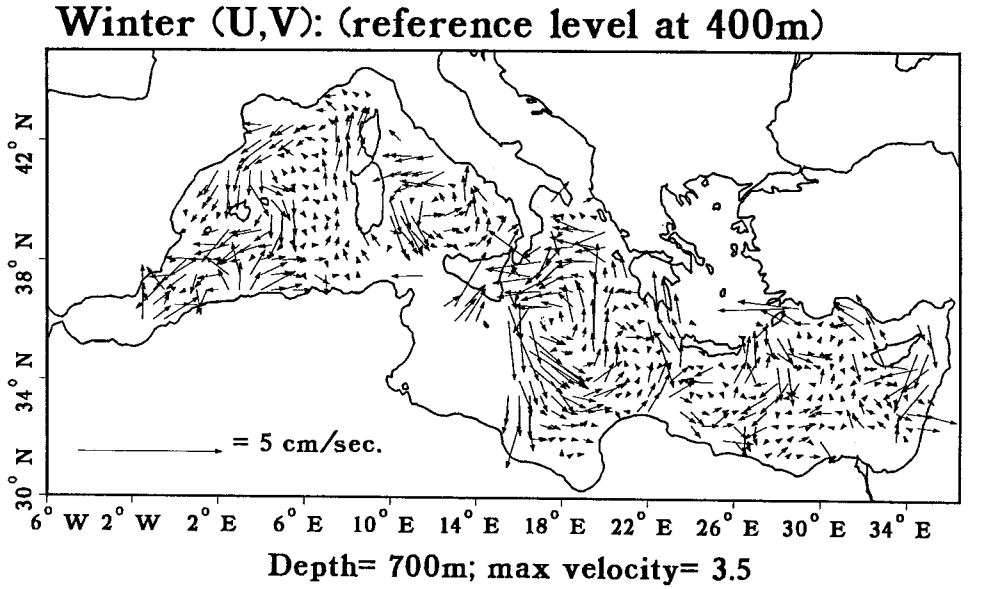

Figure 8. Winter circulation at 700 m depth, using the same inverse model as in Figure 4, except that initial level of no motion was at 400 m depth instead of 700 m.

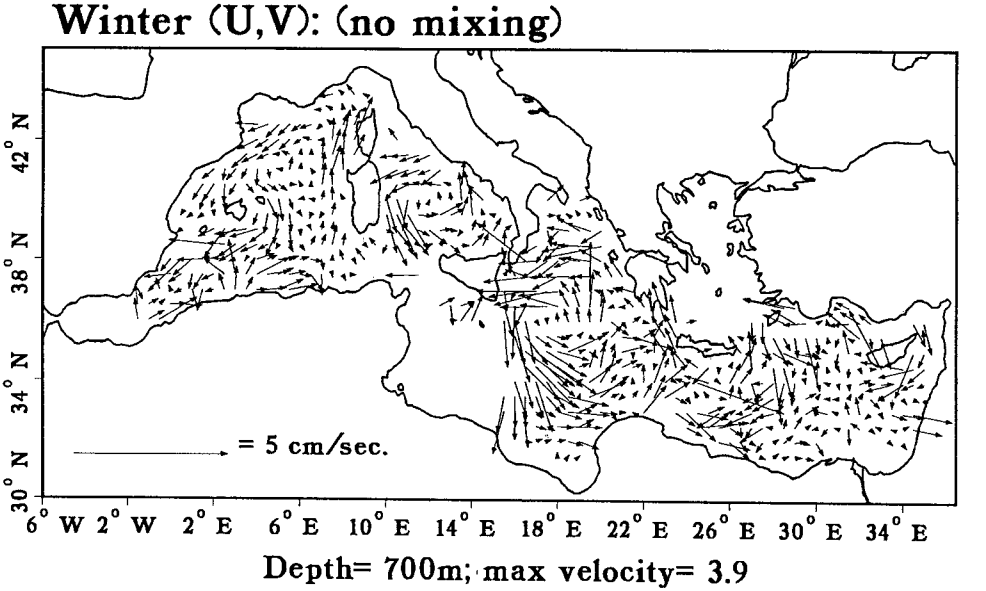

Figure 9. Winter circulation at 700 m depth, using the same inverse model as in Figure 4, except that no mixing terms were included in the temperature and salinity equations (mixing coefficients set to zero in (2)).

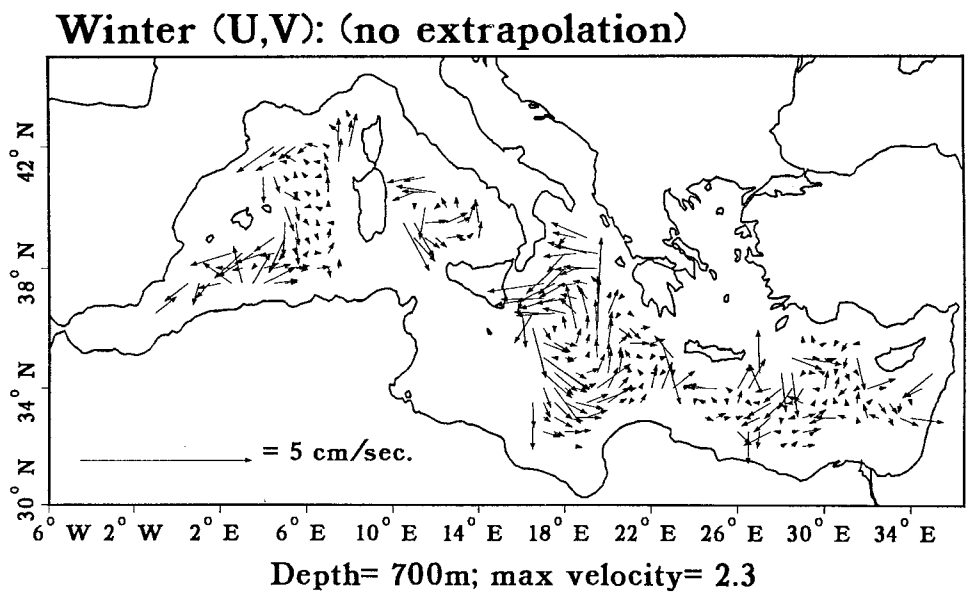

Figure 10. Winter circulation at 700 m depth, using nonextrapolated temperature and salinity data, all other inverse parameters as used to obtain the results shown in Figure 4.

as that of Figure 4, but with no mixing terms used in the temperature and salinity equations (2). Again, the deep circulation calculated by the inverse is hardly affected by the change. We have also calculated the same circulation with mixing coefficients that are constant in depth, and for a model with cross-isopycnal mixing only, and all experiments lead to the same conclusion concerning the robustness of the inverse solution for the horizontal velocity field. This is an important conclusion, as the mixing parameterization is certainly one of the dubious parts of any oceanographic model, and it is encouraging to see that the uncertainty in the mixing part of the model does not affect the calculation of the other parameters of interest. The solution for the mixing coefficients is further discussed below.

Finally, the effect of extrapolating the data to enable the calculation of the velocity near land boundaries is examined. Figure 10 shows the winter circulation at 700 m obtained from a nonextrapolated data set (with all other model parameters as in Fig. 4). Because the data are not extrapolated, center differences could not be used near land boundaries, and velocities are not calculated at grid points that are near land. One can still clearly see, however, the anticyclonic circulations in the Balearic and Tyrrhenian basins of the West Mediterranean and in the Ionian basin of the East Mediterranean. (Note that because the model is local, the velocities calculated here for the interior points are equal to those in Figure 4. The difference in the maximum velocity indicated at the bottom of the figure is due to the fact that the maximum velocities in Figure 4 occur near the grid boundaries, where they are not evaluated in

the present calculation.) In addition, we looked at the effects of smoothing the data and found that inverting the nonsmoothed data results in a noisier solution for the velocity, but the above anticyclonic features are still present.

It is especially important to demonstrate the robustness of the inverse solution for the deep velocities in the Mediterranean Sea, as the knowledge of its deep circulation is not as developed as for other parts of the world ocean. Some of the features seen in the inverse solution for the deep circulation are supported by previous evidence [such as the flow of the LIW in the Balearic basin west of Sardinia, as inferred by Wüst (1961) using the core method]. But others (deep cyclonic gyres in Ionian and Tyrrhenian basins) are not, and the robustness of the solution gives us some confidence in these interesting results.

ii. Steady state assumption. The inverse model calculates the deep reference velocities by requiring the deep (below 300 m) temperature and salinity fields to satisfy the steady state advection diffusion equations. This is done for each of the four seasonal data sets separately. For consistency, we expect the flow calculated by the inverse to be indeed steady at all four seasons. In fact, this consistency condition is satisfied by the velocities shown at 700 m, and the deep anticyclonic gyres in the West Mediterranean (Balearic and Tyrrhenian basins) and in the Ionian Sea appear almost unchanged (Figs. 4–7). We wish to emphasize that the analysis is done separately for each season, and yet the deep circulation calculated by the inverse is almost identical for all seasons.

iii. Mixing. As seen above, the form of mixing used in the model, or even its absence, does not change significantly the solution for the horizontal velocity field. The solution for the long-isopycnal mixing coefficient at a depth of 300 m for the winter season is given in Figure 11. This is the mixing coefficient calculated in the same inversion that calculated the velocities shown in Figure 4. The solution for the mixing coefficients is noisy, and seems to be controlled by the level of noise in the data. The errors calculated by the inverse for the mixing coefficients are such that the solution is not significantly different from zero in any case (similar results were obtained by Olbers *et al.* (1985) in the N. Atlantic). The noisy solution as well as the fact that it is also often negative (unless explicitly forced by inequality constraints to be positive), lead us to the conclusion that the model is unable to calculate the mixing coefficients from these data. This is not surprising, as one expects serious difficulties in calculating mixing coefficients from climatological hydrographic data (Tziperman, 1988).

The presence or absence of mixing in the model does affect the residuals in the model equations to some extent (Table 1). The addition of two mixing coefficients (long- and cross-isopycnal mixing coefficients), with three degrees of freedom for each variable (for the expansion of the vertical structure in Chebyshev polynomials, see Section 2), adds six degrees of freedom to the model, which the model uses in

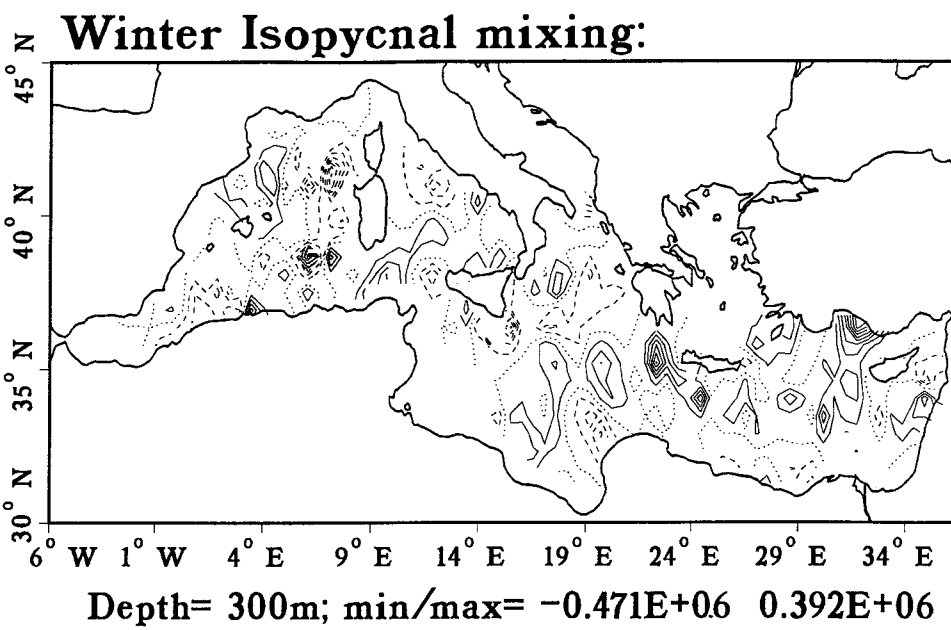

Figure 11. Solution for long isopycnal mixing coefficient at 300 m obtained by inverting the Winter data, using the same model used to calculate the velocity field of Figure 4. To help identify contour values, the zero contour was drawn using a dotted line, the positive contours with a full line, and the negative by a dash line. Contour interval is 0.02 × 10^6 cm^2/sec. Note the noisy structure of the solution, indicating that the solution for the mixing coefficients is dominated by the noise in the data.

order to reduce the residuals by about 50% on the average as compared to the model with no mixing. Yet the values of the residuals are quite acceptable even without the mixing. The small further reduction seems merely a result of artificially increasing the number of degrees of freedom of the model (from 3 to 9 unknowns), not necessarily indicating that the form of mixing used is indeed the missing physics represented by the residuals. It should be added that the failure of the model to calculate the mixing coefficients is further emphasized by the major effort required to implement the tensor diffusivities parameterization used here (Eqs. 2, 3 in Section 2).

In addition to the inability of the model to calculate mixing coefficients that are significantly different from zero, their values also strongly depend on the specific form of mixing used. When the mixing coefficients are made constant in depth, for example, (using a single term in their polynomial expansion), their values are significantly different from those obtained when allowing for depth dependence. This sensitivity to the specific form of mixing again shows that the calculated mixing parameters are controlled by the noise level in the data.

Table 1. Comparing the residuals of the temperature and salinity equations for inverse models with and without mixing terms in these equations (i.e. the inverse models used to obtain the circulation shown in Figs. 4 and 9 respectively). The residuals are calculated by substituting the inverse solution into the temperature and salinity equations (2) and calculating the resulting misfit. Shown are the horizontally averaged absolute value of the residuals, their minimum and their maximum, for three depths at which the salinity and temperature equations are used in the inverse calculation.

	T residuals			*S* residuals		
depth	min	max	avg	min	max	avg
	with mixing:					
700 m	−0.98E-01	0.61E-01	1.17E-03	−0.37E-01	0.28E-01	5.08E-04
500 m	−0.29E-01	0.50E-01	8.96E-04	−0.14E-01	0.18E-01	3.95E-04
300 m	−0.15	0.43	3.80E-03	−0.33E-01	0.70E-01	6.67E-04
	no mixing:					
700 m	−0.99E-01	0.11	3.67E-03	−0.35E-01	0.56E-01	1.22E-03
500 m	−0.41E-01	0.48E-01	1.49E-03	−0.13E-01	0.23E-01	6.00E-04
300 m	−0.63	0.40	7.91E-03	−0.65E-01	0.70E-01	1.97E-03

The values given in the table are the residuals multiplied by three months. Units are degree Celsius for temperature and ppt for salinity. The numbers may be interpreted as the change in temperature (salinity) that could be expected to occur during a three months period if the residuals were representing a term like $T_t(S_t)$ that is missing in the steady state model. For the model to be consistent, these numbers should be smaller than the actual changes that occur in the deep temperature and salinity fields of the Mediterranean Sea within a three-month period. (See Tziperman and Hecht (1988) for more details on this way of presenting the values of the residuals.)

We conclude that while mixing must be dynamically important in setting the basic vertical stratification, it is still only a second order effect (compared to horizontal advection) that cannot be calculated from our climatologically averaged hydrographic data. As long as our purpose is the calculation of the horizontal velocity field, mixing is not a crucial part of the inverse model.

iv. Parameter resolution. Every parameter calculated by the inverse model is accompanied by resolution information and an error estimate that can be used to evaluate the solution. We have clearly demonstrated the robustness of the inverse solution for the horizontal velocity in this section, and would like now to strengthen the above conclusions by briefly describing some of the resolution and error information provided by the inverse mechanism (see Wiggins (1972) for a discussion of error and resolution information that is obtained from the singular value decomposition solution).

There are nine unknowns solved for by the inverse model at each horizontal grid point (three reference velocities plus six Chebyshev coefficients for the mixing parameters). With five levels where equations for temperature and salinity are

evaluated (300, 400, 500, 600 and 700 m), the number of equations was normally 10 (except in a few shallower stations where there were fewer equations). The problem was always found to be under-determined, with the rank of the system typically equal to 5 (see TH for the criteria used to choose the rank of the matrix A in (4)). This means that at least some of the parameters were not fully resolved by the inverse.

Consider first the reference level horizontal velocities. These are found to be well resolved by the model, as indicated by the diagonal elements of the resolution matrix (typically found to be 0.95 to 1.0). In addition, the error bars calculated by the inverse for the reference velocities are on the average about 10–40% of the signal, so that these velocities are significantly different from zero.

Unlike the horizontal velocities at the reference level, the other unknowns solved for by the inverse, the mixing coefficients and vertical velocities, were not that well resolved, (diagonal elements of the resolution matrix no larger than 0.5), have large error bars (of the same order of magnitude as the solution itself), and are therefore not above the noise level. This is consistent with their having quite a random spatial structure. The difficulties with the mixing coefficients are discussed above, and the failure to properly resolve the vertical velocities is also not surprising, and was discussed in more detail by TH.

6. Conclusions

The seasonal circulation of the upper 800 m of the Mediterranean Sea was calculated from climatological data using a simple inverse model. The robustness of the inverse solution for the velocity field to various aspects of the model, such as the initial reference level used in the calculation and mixing parameterization in the temperature and salinity equations, was clearly demonstrated. The inverse results were used to address three main aspects of the general circulation of the Mediterranean Sea which are of interest, yet not sufficiently well known and understood: the seasonality of the surface circulation, the shape of the general circulation of the East Mediterranean Sea, and the shape of the deep circulation of the Mediterranean Sea.

The results show a fairly steady surface circulation in the West Mediterranean and a somewhat stronger seasonal signal in the surface circulation of the Ionian and eastern Levantine basins of the East Mediterranean. The path of the Atlantic Water in the Ionian basin forms a meander that is seen during all seasons except winter, and a small gyre in the Levantine basin south of Cyprus is also reversed during the winter season. Both of these seasonal features seem related to the change in sign of the wind curl over the East Mediterranean Sea during the winter season.

The circulation of the East Mediterranean Sea is characterized by many small sub-basin gyres which often make it difficult to distinguish transient mesoscale features from the more permanent (possibly seasonal) general circulation of the region when using quasisynoptic data. We were able to identify two small gyres calculated from our climatological data that are based on a many-year average with

features calculated from the quasi-synoptic POEM data (a gyre south-west of Cyprus and another north of the Egyptian coast), therefore indicating that these gyres are indeed part of the general circulation of the region and not transient eddies.

The use of the inverse model was particularly useful in calculating some deep features that may be difficult to calculate using an arbitrary deep level of no motion. The deep circulation was found to be steady even in regions where the upper circulation is strongly seasonal (e.g. in the Ionian basin), and shows some very interesting features in both the West and East Mediterranean extending below 500 m. In particular, the path of the high salinity Levantine Intermediate Water from the straits of Sicily toward the straits of Gibraltar is seen to pass northward along the Sardinian coast, and then south-westward along the Spanish and Majorca coasts, and not directly along the African coast. The results emphasize the need for more data of better quality in order to both further study the features seen in the deep West Mediterranean, and calculate the deep circulation of the Levantine basin of the East Mediterranean that seems to be below the noise level for the present data.

Acknowledgments. This research was supported by grant No. 87-00385 from the United States-Israel Binational Science Foundation. P.R. is supported by the National Science Foundation grant OCE-85-18487. Contribution no. 28, Department of Environmental Sciences and Energy Research, The Weizmann Institute of Science.

REFERENCES

Alain, 1960. Topographie dynamique et courants generaux dans le bassin occidental de la Mediterranee. Rev. Trav. Inst. Peches Merit., *24,* ??–??.

Anati, D. A. 1984. A dome of cold water in the Levantine basin. Deep-Sea Res., *31,* 1251–1257.

Bretherton, F. P., R. E. Davis and C. B. Famdry. 1976. A technique for objective analysis and design of oceanographic experiments applied to MODE-73. Deep-Sea Res., *23,* 559–582.

Davis, M. D., K. A. Countryman and M. J. Carron. 1986. Tailored acoustic products utilizing the NAVOCEANO GDEM (a generalized digital environmental model). A manuscript presented at the naval symposium on underwater acoustics, 1–3 April, 1986, San Diego, CA.

Hecht, A. N. Pinardi and A. R. Robinson. 1988. Currents, water masses, eddies and jets in the Mediterranean Levantine basin. J. Phys. Oceanogr., *18,* 1320–1353.

Hopkins, T. S. 1988. Physics of the Sea, *in* Western Mediterranean, key environment series, Pergamon Press, 100–125.

Malanotte-Rizzoli, P. and A. Bergamasco. 1989. The circulation of the eastern Mediterranean. Part I. Oceanologica Acta, *12,* 335–351.

Malanotte-Rizzoli, P. and A. Hecht. 1988. Large-scale properties of the eastern Mediterranean: a review. Oceanologica Acta, *11,* 323–335.

Malanotte-Rizzoli, P. and A. Robinson. 1988. P.O.E.M.: Physical oceanography of the eastern Mediterranean, the oceanography report. EOS, *69,* 14.

May, W. P. 1982. Climatological flux estimates in the Mediterranean sea: Part I. Wind and wind stress. NORDA report *54.*

Naval Oceanographic Office. 1989. Data base description for master generalized digital environmental model (GDEM). Technical report OAML-DBD-20B of the Environmental Systems Division, Stennis space center, Mississippi.

Olbers, D. J., M. Wenzel and J. Willebrand. 1985. The inference of North Atlantic circulation Patterns from climatological hydrographic data. Rev. Geophys., *23,* 313–356.

Ozsoy, E., A. Hecht and U. Unluata. 1989. Circulation and Hydrography of the Levantine Basin. Results of the POEM coordinated experiments 1985/1986. Prog. Oceanogr., *22,* 125–170.

Redi, M. H. 1982. Oceanic isopycnal mixing by coordinate rotation. J. Phys. Oceanogr., *12,* 1154–1158.

Robinson, A. R., A. Hecht, N. Pinardi, J. Bishop, W. G. Leslie, Z. Rosentroub, A. J. Mariano and S. Brenner. 1987. Small synoptic/mesoscale eddies: The energetic variability of the eastern Levantine basin. Nature, *327,* 131–134.

Tziperman, E. 1988. Calculating the time-mean oceanic general circulation and mixing coefficients from hydrographic data. J. Phys. Oceanogr., *18,* 519–525.

Tziperman, E. and A. Hecht. 1988. Circulation in the eastern Levantine basin determined by inverse methods. J. Phys. Oceanogr., *18,* 506–518.

Tziperman, E. and W. C. Thacker. 1989. An Optimal Control/Adjoint equations approach to studying the oceanic general circulation. J. Phys. Oceanogr., *19,* 1471–1485.

Wiggins, R. A. 1972. The general linear inverse problem: Implication to surface waves and free oscillations on earth structure. Rev. Geophys., *10,* 251–285.

Wunsch, C. 1978. The general circulation of the North Atlantic west of 50W determined from inverse methods. Rev. Geophys., *16,* 583–620.

Wüst, G. 1961. On the vertical circulation of the Mediterranean sea. J. Geophys. Res., *66,* 3261–3271.

Received: *1 May, 1989;* revised: *21 May, 1991.*